

**Block Copolymers**

How to cite:

International Edition: doi.org/10.1002/anie.202101102

German Edition: doi.org/10.1002/ange.202101102

# Reversible Micrometer-Scale Spiral Self-Assembly in Liquid Crystalline Block Copolymer Film with Controllable Chiral Response

Jianan Yuan, Xuemin Lu,\* Qingxiang Li, Zhiguo Lü, and Qinghua Lu\*

**Abstract:** The spiral is a fundamental structure in nature and spiral structures with controllable handedness are of increasing interest in the design of new chiroptical materials. In this study, micrometer-scale spiral structures with reversible chirality were fabricated based on the assembly of a liquid crystalline block copolymer film assisted by enantiopure tartaric acid. Mechanistic insight revealed that the formation of the spiral structures was closely related to the liquid crystalline properties of the major phase of block copolymer under the action of chiral tartaric acid. The chiral spiral structures with controllable handedness were easily erased under ultraviolet light irradiation and restored via thermal annealing. This facile thermal treatment method provides guidance for fabrication of chiral micrometer-scale spiral structures with adjustable chiral properties.

Chiral assemblies with diverse functions play important roles in nature and various physiological processes, which have inspired the scientific community to mimic these hierarchical structures using synthetic molecules. In-depth study of these chiral structures provides opportunities for the design and construction of chiral materials with excellent properties. Various chiral structures, such as helix,<sup>[1]</sup> spiral,<sup>[2]</sup> gyroid,<sup>[3]</sup> toroid,<sup>[4]</sup> and Moebius strips,<sup>[5]</sup> have been fabricated based on supramolecular assembly. Among them, the chiral spirals exhibit great sensitivity to external stimulus, just as their natural counterparts. However, the evolution of chirality and morphology from molecules to the micro-scale spiral is mysterious and it remains a challenge to construct spiral structures with controlled handedness.

Block copolymers (BCPs), composed of two or more blocks linked by chemical bonds, have been intensively investigated because of their propensity for microphase separation-induced morphology. Endowing one or two seg-

ments of BCPs with intrinsic or extrinsic chirality enables formation of different chiral assemblies ranging from nano-scale to macroscopic. For example, Ho et al. reported the formation of H\* phase by using chiral polystyrene-*b*-poly(L-lactide) under thermal annealing.<sup>[6]</sup> It is also possible to use achiral block copolymer to construct helical nanostructures by non-covalent interaction between BCPs and chiral additives.<sup>[7]</sup> Although spirals have been obtained by using achiral block copolymer under the constraint of a nanotemplate, the obtained spiral films exhibited no chirality owing to the absence of chiral tectonic units.<sup>[8]</sup> Recently, Ho et al. reported the fabrication of a spiral structure based on self-assembly of chiral block copolymer. They attributed the formation of spiral structure to chiral deformation of the layered structure.<sup>[9]</sup> However, the mechanism for spiral formation is still a black box. The construction of spiral film with controlled handedness remains challenging and hampers the in-depth understanding and functionalization of such a widely occurring natural structure. Furthermore, endowing the spiral structure with response to external stimuli is of great importance for the development of novel materials. To the best of our knowledge, no stimulus-responsive spiral has been reported until now.

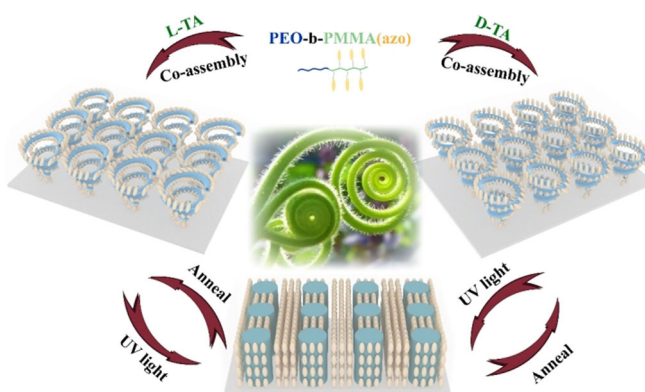
Herein, we report a facile and efficient strategy to fabricate reversible micrometer-sized three-dimensional (3D) spirals in liquid crystalline BCP (LC-BCP) film (Scheme 1). Spirals with controllable handedness were obtained by co-assembly of LC-BCP and chiral tartaric acid (TA) molecules under thermal annealing at a temperature close to the clearing point of the liquid crystal phase. Based on the liquid crystalline nature of LC-BCP and photosensitivity of the azobenzene group, the spiral structure can be easily

[\*] Dr. J. Yuan, Prof. Q. Lu  
 School of Chemical Science and Technology, Tongji University  
 Siping Road No. 1239, Shanghai, 200092 (China)  
 E-mail: qhlu@sjtu.edu.cn

Prof. X. Lu, Q. Li, Prof. Q. Lu  
 Shanghai Key Lab of Electrical & Thermal Aging, School of Chemistry and Chemical Engineering, Shanghai Jiao Tong University  
 Dongchuan Road No. 800, Shanghai, 200240 (China)  
 E-mail: xueminlu@sjtu.edu.cn

Prof. Z. Lü  
 School of Physics and Astronomy, Key Laboratory of Artificial Structures and Quantum Control, Shanghai Jiao Tong University  
 Dongchuan Road No. 800, Shanghai, 200240 (China)

Supporting information and the ORCID identification number(s) for the author(s) of this article can be found under:  
<https://doi.org/10.1002/anie.202101102>.



**Scheme 1.** Diagram showing self-assembly and reversible transformation of micrometer-scale spiral structures in LC-BCP film doped with chiral TA. Inset: Bud of *Pteridium aquilinum*.

erased by ultraviolet light irradiation and recovered by thermal annealing. This controllable self-assembly is an elegant approach for the preparation of reversible spiral structures, providing a platform to construct new chiroptical materials.

A liquid crystalline block copolymer, PEO<sub>114</sub>-PMMA(azo)<sub>46</sub>, was synthesized according to the literature.<sup>[10]</sup> The detailed procedure is provided in the Supporting Information (Figure S1). The block copolymer was composed of a poly(ethylene oxide) (PEO) segment as the minor phase segment and a liquid crystalline poly(methyl methacrylate) (PMMA)(azo) segment as the major phase. The PEO segment dispersed in the PMMA(azo) segment as a cylinder form. A solution of enantiopure D- or L-TA in tetrahydrofuran was added to a solution of LC-BCP in the same solvent. The molar ratio of PEO:TA was fixed at 1.2:1 (the relative weight ratio of TA to LC-BCP was 54 wt%). An LC-BCP film was prepared by drop-casting the mixture on a clean quartz glass slide. The obtained film was then thermally annealed for 2 h at 100 °C, close to the clearing point temperature (98 °C) of PMMA(azo)<sub>46</sub> (Supporting Information, Figure S2).

The morphology of the LC-BCP and TA hybrid film was investigated using transmission electron microscopy (TEM) and atomic force microscopy (AFM). Surprisingly, both TEM and AFM images showed micrometer-sized tubular multi-strand spiral structures with clear handedness in the annealed LC-BCP film (Figures 1 a, d and b, e). The spiral structure has a wide size distribution, the diameter of most spiral structure reached micrometer level (Supporting Information, Figure S3). The handedness of the spiral correlated with the molecular chirality of TA: a clockwise spiral structure was obtained when D-TA was used (Figure 1 c), while anticlockwise structures appeared when L-TA was used (Figure 1 f). Generally, helical nanostructures are obtained by chiral additive driven self-assembly of block copolymer, which was ascribed to chiral transfer from the chiral additive to one segment of the block copolymer.<sup>[7,11]</sup> Further investigation

based on TEM analysis indicated that the spirals were formed from a bent tube-like structure as shown in the Supporting Information, Figure S4. The inner and outer diameters of the tubular structure were ca. 10 and 38 nm, respectively. The wall of the tube-like structure was 14 nm thick, which is very close to the diameter of the PEO columnar phase before annealing (Supporting Information, inset, Figure S4c). Electron diffraction scanning (EDS) results confirmed that the dark areas in the Supporting Information, Figure S5 were mainly composed of PEO segments and the light areas were composed of PMMA(azo) segments. TEM tomography results of the spiral structure proved the three-dimensional structure of the spiral structure (Supporting Information, Figure S6). The three-dimensional spiral structures showed an average depth of 55 nm as confirmed by AFM height imaging (Supporting Information, Figure S7).

The molecular order in the spiral structure was investigated by wide-angle X-ray scattering (Figure S8a). A series of crystalline peaks were observed in enantiopure TA powder, while two sharp peaks at  $2\theta = 19^\circ$  and  $23.8^\circ$ , assigned to the crystal peaks of PEO segments, were visible in neat LC-BCP. After doping enantiopure TA, all peaks due to the individual components disappeared, while a new strong peak at  $2\theta = 16^\circ$  appeared. The absence of TA and PEO peaks indicated that no individual phase of TA or PEO was present in the LC-BCP/TA film. The new sharp peak manifests the formation of an ordered structure of the separated PEO/TA phase in the liquid phase. Combined with spot EDS results, the molecular arrangement of block copolymer in the spiral structure can be depicted as shown in the Supporting Information, Figure S8b. PEO/TA formed the outer wall and PMMA(azo)/TA formed the inner wall of the tube structure. Further assembly of these tube structures in the PMMA(azo) matrix leads to formation of the spiral structures. Based on a previous report, the TA molecules not only increase the microphase segregation tendency of block copolymer, but also provide the driving force for chiral assembly. The morphology of the block copolymer depends on the loading level of chiral molecules.<sup>[7a]</sup> To gain insight into the formation of the spiral structure, the effect of the loading level of TA molecules was investigated. As shown in the Supporting Information, Figure S9, single circular or bent tube structures were formed when the loading levels of TA were 13 wt% and 27 wt%. However, the assembled structures had no obvious handedness, irrespective of the TA chirality. Considering the difference in morphology compared with the previously reported helical structure, it is reasonable to assume that formation of the spiral structure with controlled handedness is related to the liquid crystalline properties of the PMMA(azo) segments and the interaction between TA molecules and LC-BCP.

To gain insight into the interaction between TA and LC-BCP, the circular dichroism (CD) spectra of TA-doped LC-BCP films were recorded. The corresponding UV/Vis spectra were used to confirm the peak assignments. As shown in Figure 2 a,b, new mirror signals in the range of 275–425 nm appeared after thermal annealing for 2 h, which corresponded to the characteristic adsorption of azobenzene groups. This result indicates that chirality was transferred from the small TA molecules to liquid crystalline azobenzene-containing

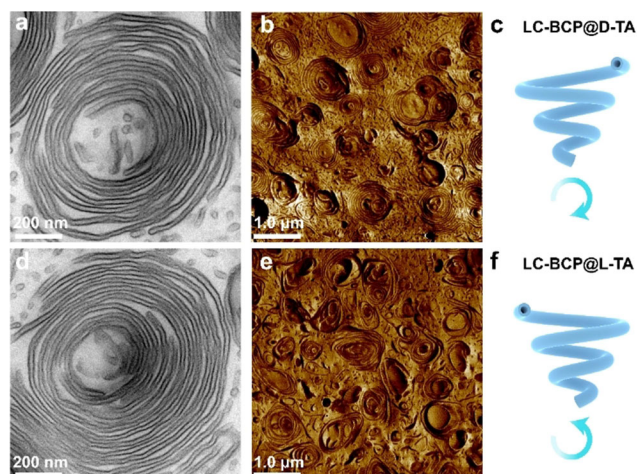


**Figure 1.** TEM and AFM images of LC-BCP films loaded with 54 wt% D-TA (a, b) and L-TA (d, e), respectively. Sketch map of spiral structures with clockwise (c) and anticlockwise (f) configurations. The slice sample was prepared by microtome with thickness of approximately 100 nm.

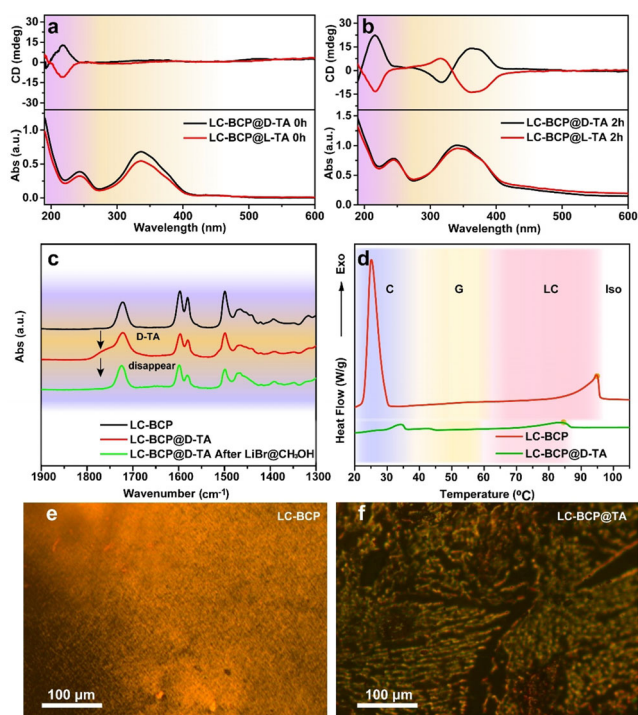


**Figure 2.** CD and UV/Vis spectra of LC-BCP film doped with 54 wt% D-TA and L-TA before (a) and after (b) thermal annealing treatment. FTIR of neat LC-BCP, LC-BCP@D-TA and LC-BCP@D-TA after removal of TA (c). DSC cooling curve of LC-BCP and LC-BCP@D-TA; C: crystalline range; G: glass transition; LC: liquid crystal phase; Iso: isotropic phase (d). POM of LC-BCP (e) at 90°C and LC-BCP@D-TA (f) at 80°C.

segments. There are two possible mechanisms for chiral transfer to the azobenzene segments: one is by interaction between the PEO/TA cylinders and the surrounding PMMA (azo) phase, and the other is by direct interaction between TA and the PMMA (azo) segments. To clarify the mechanism, homopolymer PMMA (azo) (PAZO) was used instead of LC-BCP to interact with chiral TA molecules in the same proportion. As shown in the Supporting Information, Figure S10, after annealing treatment, the CD spectra of the PAZO/TA hybrid films exhibited the same Cotton effect as those of LC-BCP/TA films. This result proved that chiral transfer can be achieved simply by the interaction between TA and PAZO, which suggests that chiral transfer in the LC-BCP/TA film might result from interaction between TA and the PMMA (azo) segments. Furthermore, in the FTIR spectra of LC-BCP film, the C=O stretching vibration peak of LC-BCP at 1721 cm<sup>-1</sup> was significantly broadened and shifted to a higher wavenumber (1760 cm<sup>-1</sup>) after TA doping. This stretching vibration peak returned to its original position after removing TA by soaking with a methanol solution of lithium bromide (Figure 2c). Based on these results, the chiral transfer can be attributed to be the result of hydrogen bonding between TA and the carbonyl group of PMMA (azo) segments.<sup>[12]</sup>

Differential scanning calorimetry (DSC) and polarizing optical microscopy (POM) were used to further assess the effect of TA doping on the liquid crystal behavior of LC-BCP/

TA hybrid film. For neat LC-BCP, the DSC profile exhibited a sharp peak at 25°C, which was attributed to the crystallization of PEO segments (Figure 2d). This peak degraded after TA doping, due to the restrictive effect of the TA-PEO hydrogen bond on the crystallization of PEO chains.<sup>[13]</sup> Furthermore, as a consequence of the TA doping, the peak corresponding to the liquid crystal clearing point of PMMA (azo) segments became weaker and reduced from 98 to 90°C (Supporting Information, Figure S2). POM observation of LC-BCP indicated different textures before and after TA doping (Figure 2e,f). A chiral pattern appeared in the POM image of LC-BCP/TA hybrid film, which indicated the change of block copolymer from achiral liquid crystal to chiral liquid crystal. Considering the effect of TA doping on the properties of PMMA (azo), it is reasonable to conclude that the chiral transfer occurred via hydrogen-bonding interaction between TA molecules and PMMA (azo) segments, leading to the change from achiral to chiral liquid crystal of the PMMA (azo) segments. Therefore, for the LC-BCP/TA hybrid film, hydrogen bonds formed not only between PEO segments and TA molecules, but also between PMMA (azo) segments and TA molecules. The hydrogen bond between PMMA (azo) segments and TA molecules drove the chiral transfer from TA molecules to the liquid crystalline PMMA (azo) segments, which caused the formation of chiral liquid crystal phase.

For the chiral BCP self-assembly under annealing, helix is the most popular structure.<sup>[7b,14]</sup> More recently, Ho et al. reported a roll-cake spiral structure in a chiral polystyrene-b-poly (L-lactide acid) film.<sup>[9]</sup> They attributed the formation of spiral structure to the self-assembly of polystyrene layer in the smectic-liquid crystal like poly (L-lactide acid) phase. The chiral structures, no matter helix or spiral (or perhaps other forms), were derived from the deformation of minor phase in BCP. Akagi et al. reported a thermally invertible chiral spiral liquid crystal field that could be used in various types of asymmetric polymerization. The chirality direction of the chiral spiral liquid crystal field determined the helicity of the synthetic polymer.<sup>[15]</sup> In BCP system, Grason et al. used the orientational self-consistent field theory to simulate the twisting self-assembly of BCP containing chiral liquid crystal units.<sup>[16]</sup> According to the second-order Frank elastic theory, there are three kinds of deformations including splaying, twisting and bending in the liquid crystal,<sup>[17]</sup> of which the twisting and bending deformations can lead to the formation of chiral structures.<sup>[9,18]</sup> Thus, the spiral structures observed here may derive from the assembly of PEO/TA segments under the chiral liquid crystal field of PMMA (azo)/TA matrix. In our case, enantiopure TA interacts with both segments, endowing the block copolymer with chirality and leading to the change of liquid crystal PMMA (azo) matrix from achiral to chiral. Subsequently, the cylinder structures that are formed by self-assembly before annealing tend to bend and twist during thermal annealing due to formation of the chiral liquid crystal field. Finally, the direction of bending of these spiral structures depends on the chirality of the liquid crystal fields. The degree of deformation of these spiral structures is dependent on the force from the chiral liquid crystal field, which is affected by the loading level of TA, annealing temperature and time.

To verify the influence of chiral liquid crystal properties of PMMA (azo)/TA, the evolution of the morphology of LC-BCP/TA film during annealing at 100 °C was tracked by TEM. As shown in Figure 3a, before annealing, the film contained irregular linear cylinders composed of PEO/TA dispersed in the PMMA (azo)/TA matrix. As thermal annealing proceeded, the cylinder structures became more regular after 15 min (Figure 3b). A twisted tube structure appeared after thermal annealing for 45 min (Figure 3c). Subsequently, the twisted tubes deformed and tended to bend in a certain direction (Figure 3d–f). After thermal annealing for 2 h, spiral structures appeared (Figure 3g). Further prolongation of thermal annealing made the spiral structures more regular. The results clearly indicate that in the early stage of thermal annealing, because the chiral liquid crystal phase of PMMA (azo)/TA does not form completely, only cylinder structures appear due to microphase separation of block copolymers. Further extending the thermal annealing time allows the chiral liquid crystal phase of PMMA (azo)/TA to form. In the chiral liquid crystal matrix, the tube structures tend to be bent and twisted owing to the twisting force from the chiral liquid crystal PMMA (azo)/TA matrix, finally leading to the formation of 3D micrometer-sized spiral structures (Figure 3i). Because the rotational direction of the resultant chiral liquid crystal depends on the chirality of the dopant, the handedness of the 3D spiral structure is regulated by chiral additives. The stability of the spiral structure was further investigated by varying the annealing time. As shown in the Supporting Information, Figure S11a, the spiral morphology

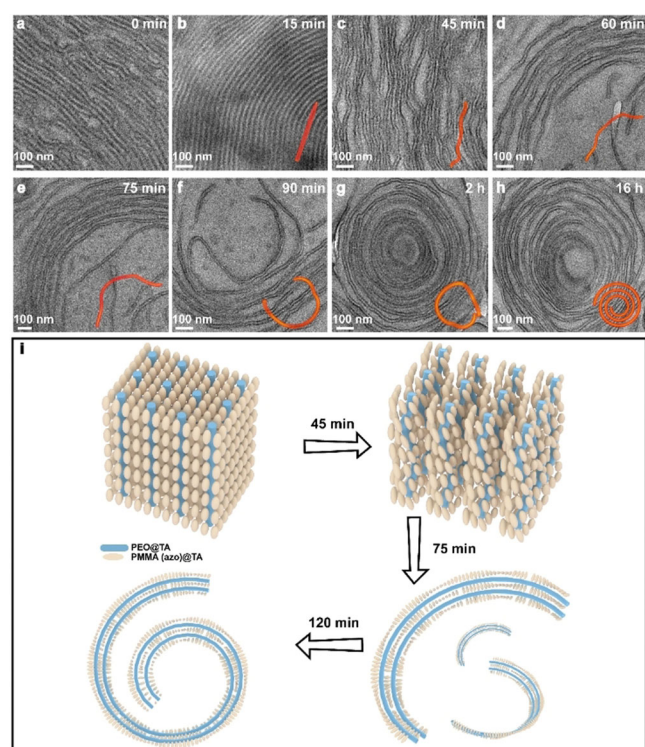


**Figure 3.** a)–h) TEM images of the structural evolution of LC-BCP film doped with 54 wt % L-TA during annealing (100 °C) at a) 0 min, b) 15 min, c) 45 min, d) 60 min, e) 75 min, f) 90 min, g) 2 h and h) 16 h; i) Diagram of structural evolution.

in the hybrid film remained unchanged after thermal annealing at 100 °C for 3 days. We also found that no obvious change of the spiral structures occurred when the sample was kept at room temperature for one year (Supporting Information, Figure S11b). These results proved that the spirals formed in the hybrid film was thermodynamic stable.

Chirality and liquid crystal properties of LC-BCP/TA play a key role in the formation of spiral structures, which can be confirmed by the following facts. When the LC-BCP/TA film was thermally annealed at 60 °C, no spiral structure appeared even when the annealing time was increased to 16 h. This is because the chiral liquid crystal state cannot be formed at 60 °C (Supporting Information, Figure S12). On the other hand, when racemic TA was used as chiral additive instead of enantiopure TA, as shown in the Supporting Information, Figure S13, no spiral structure appeared in the LC-BCP/TA hybrid film. The azobenzene groups in the liquid crystal unit can also be used to mediate the response of the spiral structure to external light stimulus. In this work, the LC-BCP film containing micrometer-scale spiral structures was exposed to ultraviolet light at 365 nm. We found that both the CD signals attributed to the azobenzene group and the spiral structures disappeared after ultraviolet irradiation for 30 s (Figure 4). This is due to isomerization of the azobenzene group, from trans-state to cis-state, which affects the regular arrangement of the azobenzene-containing side chains and disrupts the liquid crystal phase of PMMA (azo) blocks as shown in Figure 4g. Consequently, the effect of the chiral liquid crystal field on the PEO/TA cylinders is weakened, leading to disassembly of the spiral structures. However, when the cis-azobenzene was annealed and returned to the trans-azobenzene, the chiral liquid crystal performance of PMMA

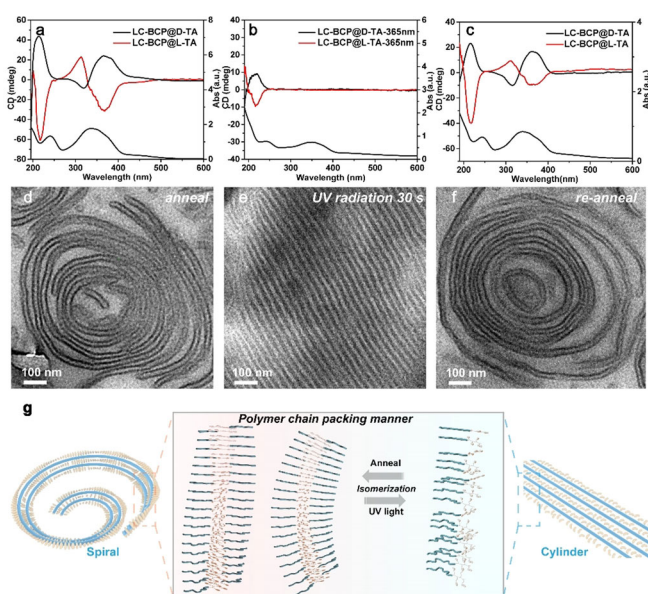


**Figure 4.** a)–c) CD spectra (containing UV/Vis spectra) and d)–f) TEM images of annealed LC-BCP film doped with 54 wt % L-TA before (a, d) and after (b, e) UV irradiation (30 s, 365 nm, 150 mW cm<sup>-2</sup>), and the restoration of the spiral structure after re-annealing for 2 h (c, f); g) Diagram of the structural change induced by UV irradiation and thermal recovery.

(azo)/TA could be recovered (Figure 4c).<sup>[19]</sup> Furthermore, the spiral structure of the film can also be reversibly tuned (Figure 4f). This discovery will bring new opportunities for research on chiral spirals and their application.

In summary, we have demonstrated a facile method for fabricating micrometer-scale spiral structures with controllable handedness using LC-BCP film doped with chiral TA. A mechanism for formation of the spiral structures is proposed based on the principle of bending and twisting of the chiral liquid crystal towards PEO/TA columns. The chiral liquid crystal field plays a decisive role in self-assembly of the spiral structures. The micrometer-scale spiral structures and chiral optical properties exhibit light-responsive erasure and thermal regeneration behavior. The approach presented here could also be extended to other liquid crystal block copolymers and may open a new route to develop advanced chiral materials for cryptography.

### Acknowledgements

This work was financially supported by the National Natural Science Foundation of China (grant nos. 21574081, 21975156 and 51733007). X.L. thanks Prof. Ming Li at Shanghai Jiao Tong University for the discussion on the mechanism of spiral formation. J.Y. thanks Dr. Q Deng and Prof. Lu Han at Tongji University for the discussion on 3D tomography of spiral structure.

### Conflict of interest

The authors declare no conflict of interest.

**Keywords:** block copolymers · chirality · self-assembly · spiral structures

- [1] a) G. Liu, J. Sheng, H. Wu, C. Yang, G. Yang, Y. Li, R. Ganguly, L. Zhu, Y. Zhao, *J. Am. Chem. Soc.* **2018**, *140*, 6467–6473; b) H. Liu, B. Pang, R. Garces, R. Dervisoglu, L. Chen, L. Andreas, K. Zhang, *Angew. Chem. Int. Ed.* **2018**, *57*, 16323–16328; *Angew. Chem.* **2018**, *130*, 16561–16566.
- [2] N. Sasaki, M. F. J. Mabeoone, J. Kikkawa, T. Fukui, N. Shioya, T. Shimoaka, T. Hasegawa, H. Takagi, R. Haruki, N. Shimizu, S.-i. Adachi, E. W. Meijer, M. Takeuchi, K. Sugiyasu, *Nat. Commun.* **2020**, *11*, 3578.

- [3] a) C. Chen, R. Kieffer, H. Ebert, M. Prehm, R.-b. Zhang, X. Zeng, F. Liu, G. Ungar, C. Tschierske, *Angew. Chem. Int. Ed.* **2020**, *59*, 2725–2729; *Angew. Chem.* **2020**, *132*, 2747–2751; b) N. Uemura, T. Kobayashi, S. Yoshida, Y.-x. Li, K. Goossens, X. Zeng, G. Watanabe, T. Ichikawa, *Angew. Chem. Int. Ed.* **2020**, *59*, 8445–8450; *Angew. Chem.* **2020**, *132*, 8523–8528.
- [4] P. Xu, L. Gao, C. Cai, J. Lin, L. Wang, X. Tian, *Angew. Chem. Int. Ed.* **2020**, *59*, 14281–14285; *Angew. Chem.* **2020**, *132*, 14387–14391.
- [5] a) Z. Geng, B. Xiong, L. Wang, K. Wang, M. Ren, L. Zhang, J. Zhu, Z. Yang, *Nat. Commun.* **2019**, *10*, 4090; b) G. Ouyang, L. Ji, Y. Jiang, F. Würthner, M. Liu, *Nat. Commun.* **2020**, *11*, 5910.
- [6] a) Y. W. Chiang, R. M. Ho, B. T. Ko, C. C. Lin, *Angew. Chem. Int. Ed.* **2005**, *44*, 7969–7972; *Angew. Chem.* **2005**, *117*, 8183–8186; b) R. M. Ho, Y. W. Chiang, C. K. Chen, H. W. Wang, H. Hasegawa, S. Akasaka, E. L. Thomas, C. Burger, B. S. Hsiao, *J. Am. Chem. Soc.* **2009**, *131*, 18533–18542.
- [7] a) X. Lu, J. Li, D. Zhu, M. Xu, W. Li, Q. Lu, *Angew. Chem. Int. Ed.* **2018**, *57*, 15148–15152; *Angew. Chem.* **2018**, *130*, 15368–15372; b) L. Yao, X. Lu, S. Chen, J. J. Watkins, *Macromolecules* **2014**, *47*, 6547–6553.
- [8] a) J. Chai, J. M. Buriak, *ACS Nano* **2008**, *2*, 489–501; b) H. K. Choi, J.-B. Chang, A. F. Hannon, J. K. W. Yang, K. K. Berggren, A. Alexander-Katz, C. A. Ross, *Nano Futures* **2017**, *1*, 015001.
- [9] K.-C. Yang, R.-M. Ho, *ACS Macro Lett.* **2020**, *9*, 1130–1134.
- [10] Y. Tian, K. Watanabe, X. Kong, J. Abe, T. Iyoda, *Macromolecules* **2002**, *35*, 3739–3747.
- [11] X. Lu, D.-p. Song, A. Ribbe, J. J. Watkins, *Macromolecules* **2017**, *50*, 5293–5300.
- [12] B. Su, S. Wang, Y. Wu, X. Chen, Y. Song, L. Jiang, *Adv. Mater.* **2012**, *24*, 2780–2785.
- [13] L. Yao, J. J. Watkins, *ACS Nano* **2013**, *7*, 1513–1523.
- [14] H.-F. Wang, K.-C. Yang, W.-C. Hsu, J.-Y. Lee, J.-T. Hsu, G. M. Grason, E. L. Thomas, J.-C. Tsai, R.-M. Ho, *Proc. Natl. Acad. Sci. USA* **2019**, *116*, 4080–4089.
- [15] K. Akagi, T. Yamashita, K. Horie, M. Goh, M. Yamamoto, *Adv. Mater.* **2020**, *32*, 1906665.
- [16] W. Zhao, T. P. Russell, G. M. Grason, *Phys. Rev. Lett.* **2013**, *110*, 058301.
- [17] G. M. Grason, *Soft Matter* **2020**, *16*, 1102–1116.
- [18] D. M. Hall, I. R. Bruss, J. R. Barone, G. M. Grason, *Nat. Mater.* **2016**, *15*, 727–732.
- [19] a) X. Cheng, T. Miao, L. Yin, Y. Ji, Y. Li, Z. Zhang, W. Zhang, X. Zhu, *Angew. Chem. Int. Ed.* **2020**, *59*, 9669–9677; *Angew. Chem.* **2020**, *132*, 9756–9764; b) L. Yin, M. Liu, Y. Zhao, S. Zhang, W. Zhang, Z. Zhang, X. Zhu, *Polym. Chem.* **2018**, *9*, 769–776.

Manuscript received: January 24, 2021

Revised manuscript received: March 9, 2021

Accepted manuscript online: March 21, 2021

Version of record online: ■■■■■■

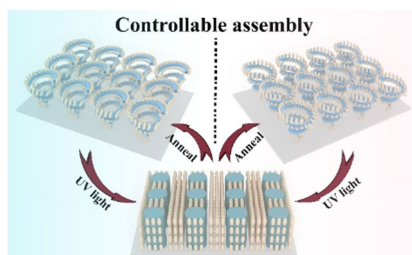
## Communications

## Block Copolymers

J. Yuan, X. Lu,\* Q. Li, Z. Lü,

Q. Lu\*     

Reversible Micrometer-Scale Spiral Self-Assembly in Liquid Crystalline Block Copolymer Film with Controllable Chiral Response



Micrometer-scale spiral structures with clear handedness are obtained through self-assembly of liquid crystalline block copolymer, poly(ethylene oxide)-*b*-poly(methyl methacrylate) bearing azobenzene mesogen side chains, with the aid of enantiopure tartaric acid as chiral additive. The formation of spiral structures can be reversibly controlled by ultraviolet light and heat treatment.